Simultaneous measurement of the electronic and lattice temperatures in GaAs/$Al_{0.45}Ga_{0.55}As$ quantum-cascade lasers: Influence on the optical performance

Vincenzo Spagnolo[a)]
INFM Regional Laboratory LIT³ and Dipartimento Interateneo di Fisica, Politecnico di Bari Via Amendola 173, 70126 Bari, Italy

Gaetano Scamarcio[b)]
INFM Regional Laboratory LIT³ and Dipartimento Interateneo di Fisica, Università di Bari Via Amendola 173, 70126 Bari, Italy

Hideaki Page and Carlo Sirtori
Thales Research and Technology, 91404 Orsay Cedex, France

(Received 24 November 2003; accepted 17 March 2004; published online 20 April 2004)

We measured the electronic and lattice temperatures in steady-state operating GaAs/AlGaAs quantum-cascade lasers, by means of microprobe band-to-band photoluminescence. Thermalized hot-electron distributions with temperatures up to 800 K are established. The comparison of our data with the analysis of the temperature dependence of device optical performances shows that the threshold current is determined by the lattice temperature. © *2004 American Institute of Physics.* [DOI: 10.1063/1.1739518]

Quantum-cascade lasers (QCLs) are unipolar devices based on transitions between intersubband states created by quantum confinement in ultrathin alternating layers of semiconductors. The emission wavelength is determined via the proper choice of well and barrier layers thickness and by tailoring the optical matrix elements and the relaxation times. Laser emission has been reported in the midinfrared wavelengths (3.5–24 μm) and recently also in the terahertz range (67–100 μm).[1–5] The demonstration of continuous-wave (cw) operation at room temperature in InP-based QCLs using a buried waveguide[6] confirms the high potential of QCLs for applications including gas sensing and wireless communications.[7] However, high-temperature cw operation over a large range of wavelengths remains the most important performance milestone for the wider commercialization of these laser sources. This, in turn, requires further progress in the device design to reduce the threshold current and its temperature sensitivity. Thermally induced leakage of electrons into delocalized continuumlike states is the main process controlling the temperature dependence of the threshold current density. This process reduces the injection efficiency into the upper laser level and contributes to the establishment of a nonequilibrium electronic distribution, which may weaken the population inversion.[8]

In this work, we report the simultaneous determination of electronic and lattice temperatures in operating GaAs/AlGaAs QCLs under steady-state operation, by means of a noninvasive microprobe band-to-band photoluminescence (PL) technique. Our results demonstrate the establishment of a thermalized hot-electron distribution. Comparison with optical power–current characteristics as a function of the actual active region temperature shows that the threshold current is determined by the active region lattice temperature. These results validate a method based on the analysis of light–current and current–voltage characteristics to determine the device thermal resistance and active region temperatures.

GaAs/$Al_{0.45}Ga_{0.55}As$ QCLs were grown by molecular-beam epitaxy on GaAs substrates *n*-doped to $2-3\times10^{18}$ cm^{-3}. The active layer consists of a 1.63 μm thick region composed of 36 periods of a GaAs/$Al_{0.45}Ga_{0.55}As$ heterostructure designed for emission at $\lambda=9.0$ μm. The midinfrared optical performance and electrical characteristics of the devices have been reported elsewhere.[9] Essential features are a diagonal anticrossed laser transition and depopulation of the laser ground state via resonant optical phonon emission and tunneling into the injector. The active layer is sandwiched by two 3.5 μm thick GaAs layers *n* doped to 8×10^{16} cm^{-3} and two 1 μm thick GaAs plasmon cladding layers heavily *n* doped to 5×10^{18} cm^{-3}. Ridge waveguides 2 mm long and 30 μm wide were defined using photolithographic techniques and wet chemical etching. Two 10 μm deep semicircular trenches were wet etched through the active region to define the laser ridge and ion implantation was used to electrically isolate the regions bordering the laser ridge. The devices were mounted on the cold finger of a helium flow microcryostat using thermal grease to facilitate thermal contact. The heat sink temperature was controlled by a Si-diode mounted close to the laser. The microprobe apparatus used for PL measurements is described in detail in Ref. 10. The 476.2 nm line of a Kr^+ laser was focused to a 1 μm spot onto the laser front facet. Laser-induced heating of the samples was avoided keeping the incident power density $<10^4$ W/cm^2.

The active region local lattice temperature (T_L) has been obtained by comparing the PL peak energy shift induced by heating with a calibration curve obtained by probing the device at zero current while varying the heat sink temperature,

a)Electronic mail: spagnolo@fisica.uniba.it
b)Electronic mail: scamarcio@fisica.uniba.it

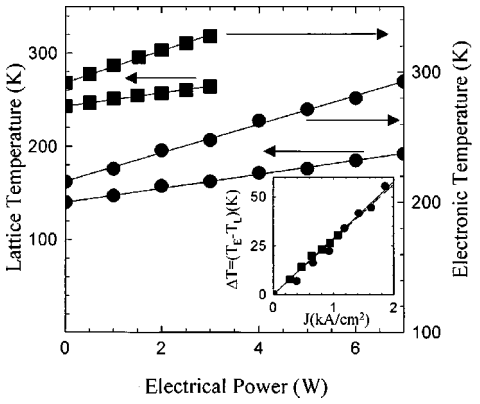

FIG. 1. Mean lattice temperature and electronic temperature in the active region of the investigated $GaAs/Al_{0.45}Ga_{0.55}As$ QCL as a function of the electrical power measured at a heat sink temperature of $T_H=140$ K (●) and $T_H=243$ K (■). The lines are linear fits to the data. The slopes of the lattice temperatures give the thermal resistance values $R=7.6$ K/W at $T_H=140$ K and $R=7.2$ K/W at $T_H=243$ K. Inset: Electronic temperature increase with respect to the lattice temperature as a function of the current density measured at $T_H=140$ K (● symbols) and $T_H=243$ K (■ symbols). For the electronic temperatures, an offset value of 25 K at $T_H=243$ K and 22.7 K at $T_H=140$ K is used in order to take into account the heating of the electronic ensemble induced by the probe Kr^+ laser (see Ref. 13). The slope of the linear fit gives the electron–lattice coupling constant: $\alpha_{E-L}=27.0$ K/(kA cm^2) at 140 K; $\alpha_{E-L}=28.8$ K/(kA cm^2) at $T_H=243$ K.

following the method outlined in Ref. 11. Self-consistent band structure calculations show that the PL emission is dominated by a transition involving the lower confined level of the conduction band in the active layer. The analysis of the high-energy slope of the PL band yields the electronic temperature (T_E) in the active region.[12]

Figure 1 shows the temperatures T_L and T_E measured in the active region, at a heat sink temperature of $T_H=243$ K and $T_H=140$ K, as a function of the cw electrical power up to 7 W, below laser threshold. Both T_L and T_E show a linear dependence with the electrical power, although the proportionality constant is significantly different. The slope of the lattice temperature gives the device thermal resistance values $R=7.2$ K/W at $T_H=243$ K, and $R=7.6$ K/W at $T_H=140$ K.[11,12] The electronic temperature slope slightly decreases from $R_E=17.1$ K/W at $T_H=243$ K to $R_E=15.3$ K/W at $T_H=140$ K. The difference between T_E and T_L at zero current is expected and ascribed to the heating of the electronic ensemble due to the large excess energy of the electron–hole pairs excited by the probe Kr^+ laser. The fact that R_E is significantly larger than R shows that the electron–phonon interaction is not large enough to efficiently dissipate the relatively large amount of electrical power via optical–phonon emission.

The inset of Fig. 1 shows the difference between the electronic and lattice temperatures in the active region as a function of the injected current density J, at a fixed heat sink temperature of $T_H=243$ K and $T_H=140$ K. A linear correlation between ΔT and J is found. This trend confirms the establishment of a thermalized hot-electron energy distribution, and the proportionality constant $\alpha_{E-L}=\Delta T/J$ is a measure of the electron–lattice coupling.[13,14]

Figure 2(a) shows the light-current and voltage-current characteristics in pulsed mode obtained at different heat sink temperatures, using a short pulse width (45 ns) and a very low duty cycle ($\delta=0.09\%$). Under these conditions, self-heating effects are negligible and the heat sink temperature approaches that of the active region. Figure 2(b) shows the threshold current density as a function of the active region temperature.

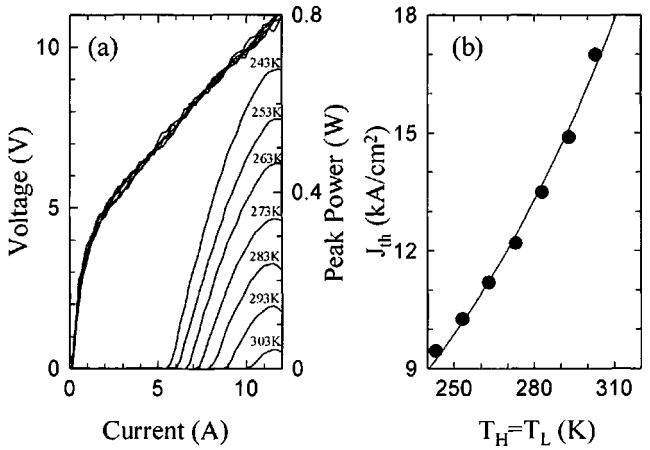

FIG. 2. (a) Light–current–voltage characteristics of the investigated $GaAs/Al_{0.45}Ga_{0.55}As$ QCL obtained at low duty cycle (pulse width=45 ns, repetition rate=20 kHz), as a function of the heat sink temperature. Note that the current–voltage characteristics are practically unchanged in the range of 243 K–303 K. Light from one laser facet was collected using $f/0.8$ optics and a calibrated room-temperature mercury–cadmium–telluride detector. The estimated collection efficiency is $\eta=0.5$. (b) Temperature dependence of the threshold current density. The solid line reproduces the typical exponential dependence $J_{th}=J_0\exp(T/T_0)$, with $T_0=100$ K.

At larger duty cycles, the active region temperature significantly deviates from T_H due to self-heating. This is evident in Fig. 3(a) showing the light–current characteristics as a function of the duty cycle up to $\delta=5.2\%$. In this case, we estimate the active region temperature at threshold from Fig. 2(b), using J_{th} as a thermometric property. These temperatures are plotted in Fig. 3(b), as a function of the electrical power at threshold $P_{th}=I_{th}\cdot V_{th}\cdot\delta$, where V_{th} is taken from the current–voltage characteristics of Fig. 2(a). The observed linear dependence corresponds to a thermal resistance of 6.9 K/W, which coincides with the value obtained by PL measurements (see Fig. 1). This shows that the analysis of light–

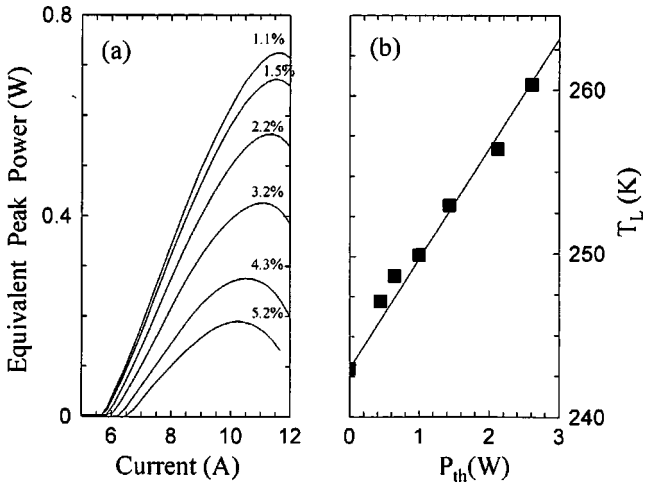

FIG. 3. (a) Pulsed light–current characteristics of the investigated $GaAs/Al_{0.45}Ga_{0.55}As$ QCL obtained at constant heat sink temperature $T_H=243$ K, as a function of the duty cycle up to 5.2%, with a pulsed width of 45 ns. (b) Mean lattice temperature of the active region, extracted from the threshold current values of (a), as a function of the electrical power. The linear fit corresponds to a thermal resistance of 6.9 K/W.

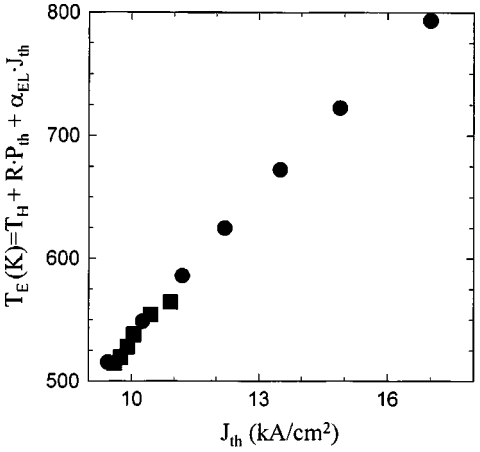

FIG. 4. Mean electronic temperature of the active region as a function of the threshold current density, obtained at a low (●) and high duty cycle (■).

current–voltage characteristics can be used as an alternative method to determine thermal resistance and active region temperature in QCLs.

In order to assess the electronic temperature under pulsed mode operation, we use the relation $T_E = T_H + R \cdot P_{\text{th}} + \alpha_{E-L} \cdot J_{\text{th}}$. The obtained T_E values, plotted as a function of J_{th} in Fig. 4, show that the electronic temperature at threshold can be as high as ~800 K (around $T_L = 300$ K), in agreement with recent Monte Carlo calculations.[15] These findings support the explanation of the thermal deterioration of optical performance of QCLs [see Figs. 2(a) and 3(a)] in terms of gain broadening and reduction of the injection efficiency as a consequence of carrier leakage out of the active region. Similar processes are expected to be particularly important also for THz QCLs, in which the energy relaxation via electron–electron scattering plays a central role and larger values of α_{E-L} can be predicted.

This work was partly supported by MIUR, project P5WP2 cluster 26 "Materiali Innovativi," project FIRB-RBAU01E8SS, the European Union via the SUPERSMILE Project IST-1999-14193, and the ANSWER Project STRP 505642-1.

[1] C. Gmachl, F. Capasso, D. L. Sivco, and A. Y. Cho, Rep. Prog. Phys. **64**, 1533 (2001).
[2] C. Sirtori, H. Page, and C. Becker, Philos. Trans. R. Soc. London, Ser. A **359**, 505 (2001).
[3] R. Kohler, A. Tredicucci, F. Beltram, H. W. Beere, E. H. Linfield, A. G. Davies, D. A. Ritchie, R. C. Iotti, and F. Rossi, Nature (London) **417**, 156 (2002).
[4] M. Rochat, L. Ajili, H. Willenberg, J. Faist, H. E. Beere, A. G. Davies, E. H. Linfield, and D. Ritchie, Appl. Phys. Lett. **81**, 1381 (2002).
[5] B. S. Williams, H. Callebaut, S. Kumar, Q. Hua, and J. L. Reno, Appl. Phys. Lett. **82**, 1015 (2003).
[6] M. Beck, D. Hofstetter, T. Aellen, J. Faist, U. Oesterle, M. Ilegems, E. Gini, and H. Melchior, Science **295**, 301 (2002).
[7] F. Capasso, R. Paiella, R. Martini, R. Colombelli, C. Gmachl, T. L. Myers, M. S. Taubman, R. M. Williams, C. G. Bethea, K. Unterrainer, H. Y. Hwang, D. L. Sivco, A. Y. Cho, A. M. Sergent, H. C. Liu, and E. A. Whittaker, IEEE J. Quantum Electron. **38**, 511 (2002).
[8] C. Sirtori, H. Page, C. Becker, and V. Ortiz, IEEE J. Quantum Electron. **38**, 547 (2002).
[9] H. Page, C. Becker, A. Robertson, G. Glastre, V. Ortiz, and C. Sirtori, Appl. Phys. Lett. **78**, 3259 (2001).
[10] V. Spagnolo, M. Troccoli, G. Scamarcio, C. Gmachl, F. Capasso, A. Tredicucci, A. M. Sergent, A. L. Hutchinson, D. L. Sivco, and A. Y. Cho, Appl. Phys. Lett. **78**, 2095 (2001).
[11] V. Spagnolo, M. Troccoli, G. Scamarcio, C. Becker, G. Glastre, and C. Sirtori, Appl. Phys. Lett. **78**, 1177 (2001).
[12] See, e.g., J. Shah, *Hot Carriers in Semiconductor Nanostructures: Physics and Applications* (Academic, New York, 1992).
[13] S. Lurji, in *Hot Electron in Semiconductor: Physics and Devices*, edited by N. Balkan (Clarendon, Oxford, 1998).
[14] P. Harrison, D. Indjin, and R. W. Kelsall, J. Appl. Phys. **92**, 6921 (2002).
[15] R. C. Iotti and F. Rossi, Appl. Phys. Lett. **78**, 2902 (2001).